FirstPage

Pure Spin Current Injection in Hydrogenated Graphene Structures

Reinaldo Zapata-Peña[1], Bernardo S. Mendoza[1], Anatoli I. Shkrebtii[2]

[1] *Centro de Investigaciones en Óptica, León, Guanajuato 37150, México and*

[2] *University of Ontario, Institute of Technology, Oshawa, ON, L1H 7L7, Canada*

(Dated: May 23, 2017)

Lorem ipsum dolor sit amet, consectetuer adipiscing elit. Etiam lobortis facilisis sem. Nullam nec mi et neque pharetra sollicitudin. Praesent imperdiet mi nec ante. Donec ullamcorper, felis non sodales commodo, lectus velit ultrices augue, a dignissim nibh lectus placerat pede. Vivamus nunc nunc, molestie ut, ultricies vel, semper in, velit. Ut porttitor. Praesent in sapien. Lorem ipsum dolor sit amet, consectetuer adipiscing elit. Duis fringilla tristique neque. Sed interdum libero ut metus. Pellentesque placerat. Nam rutrum augue a leo. Morbi sed elit sit amet ante lobortis sollicitudin. Praesent blandit blandit mauris. Praesent lectus tellus, aliquet aliquam, luctus a, egestas a, turpis. Mauris lacinia lorem sit amet ipsum. Nunc quis urna dictum turpis accumsan semper.

I. INTRODUCTION

Lorem ipsum dolor sit amet, consectetuer adipiscing elit. Etiam lobortis facilisis sem. Nullam nec mi et neque pharetra sollicitudin. Praesent imperdiet mi nec ante. Donec ullamcorper, felis non sodales commodo, lectus velit ultrices augue, a dignissim nibh lectus placerat pede. Vivamus nunc nunc, molestie ut, ultricies vel, semper in, velit. Ut porttitor. Praesent in sapien. Lorem ipsum dolor sit amet, consectetuer adipiscing elit. Duis fringilla tristique neque. Sed interdum libero ut metus. Pellentesque placerat. Nam rutrum augue a leo. Morbi sed elit sit amet ante lobortis sollicitudin. Praesent blandit blandit mauris. Praesent lectus tellus, aliquet aliquam, luctus a, egestas a, turpis. Mauris lacinia lorem sit amet ipsum. Nunc quis urna dictum turpis accumsan semper. Lorem ipsum dolor sit amet, consectetuer adipiscing elit. Etiam lobortis facilisis sem. Nullam nec mi et neque pharetra sollicitudin. Praesent imperdiet mi nec ante. Donec ullamcorper, felis non sodales commodo, lectus velit ultrices augue, a dignissim nibh lectus placerat pede. Vivamus nunc nunc, molestie ut, ultricies vel, semper in, velit. Ut porttitor. Praesent in sapien. Lorem ipsum dolor sit amet, consectetuer adipiscing elit. Duis fringilla tristique neque. Sed interdum libero ut metus. Pellentesque placerat. Nam rutrum augue a leo.

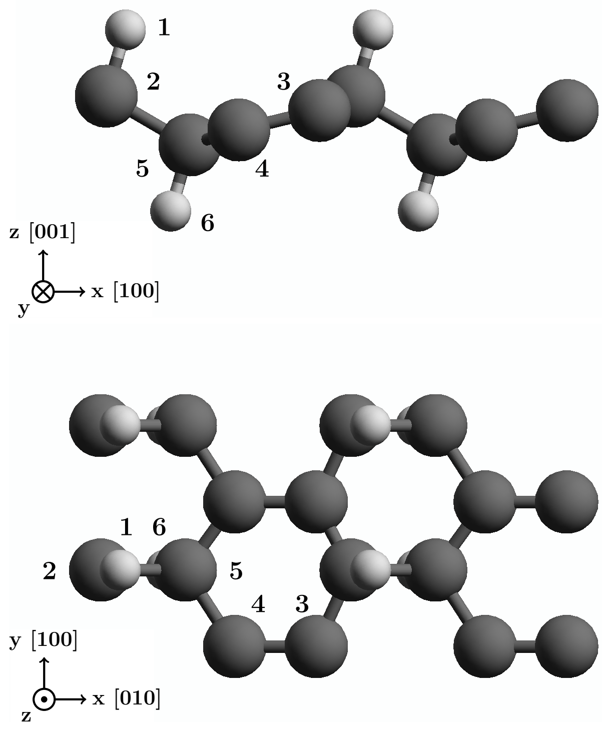

FIG. 1. Alt structure`fig:alt-struc`

Morbi sed elit sit amet ante lobortis sollicitudin. Praesent blandit blandit mauris. Praesent lectus tellus, aliquet aliquam, luctus a, egestas a, turpis. Mauris lacinia lorem sit amet ipsum. Nunc quis urna dictum turpis accumsan semper.

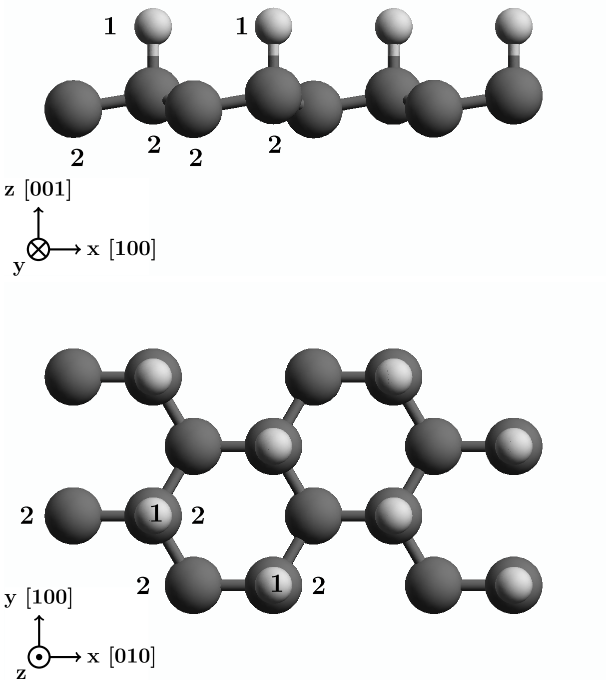

FIG. 2. Up structure fig:up-struc

Lorem ipsum dolor sit amet, consectetuer adipiscing elit. Etiam lobortis facilisis sem. Nullam nec mi et neque pharetra sollicitudin. Praesent imperdiet mi nec ante. Donec ullamcorper, felis non sodales commodo, lectus velit ultrices augue, a dignissim nibh lectus placerat pede. Vivamus nunc nunc, molestie ut, ultricies vel, semper in, velit. Ut porttitor. Praesent in sapien. Lorem ipsum dolor sit amet, consectetuer adipiscing elit. Duis fringilla tristique neque. Sed interdum libero ut metus. Pellentesque placerat. Nam rutrum augue a leo. Morbi sed elit sit amet ante lobortis sollicitudin. Praesent blandit blandit mauris. Praesent lectus tellus, aliquet aliquam, luctus a, egestas a, turpis. Mauris lacinia lorem sit amet ipsum. Nunc quis urna dictum turpis accumsan semper.

Lorem ipsum dolor sit amet, consectetuer adipiscing elit. Etiam lobortis facilisis sem. Nullam nec mi et neque pharetra sollicitudin. Praesent imperdiet mi nec ante. Donec ullamcorper, felis non sodales commodo, lectus velit ultrices augue, a dignissim nibh lectus placerat pede. Vivamus nunc nunc, molestie ut, ultricies vel, semper in, velit. Ut porttitor. Praesent in sapien. Lorem ipsum dolor sit amet, consectetuer adipiscing elit. Duis fringilla tristique neque. Sed interdum libero ut metus. Pellentesque placerat. Nam rutrum augue a leo. Morbi sed elit sit amet ante lobortis sollicitudin. Praesent blandit blandit mauris. Praesent lectus tellus, aliquet aliquam, luctus a, egestas a, turpis. Mauris lacinia lorem sit amet ipsum. Nunc quis urna dictum turpis accumsan semper.

II. THEORY

sec:theory

A. Pure spin velocity

sec:theory-pure_spin_current

The spin density injection current $\dot{K}^{\mathrm{ab}}$ can be written in terms of a material response pseudotensor $\mu^{\mathrm{abcd}}(\omega)$ as

$$\dot{K}^{\mathrm{ab}}(\omega) = \mu^{\mathrm{abcd}}(\omega) E^{\mathrm{c}}(\omega) E^{\mathrm{d}*}(\omega)$$

where the roman superscripts denote Cartesian components corresponding a to the spin velocity direction and b to the spin polarization direction and the pseudotensor can be written as

$$\mu^{\mathrm{abcd}}(\omega) = \frac{\pi e^2}{\hbar^2} \int \frac{d^3K}{8\pi^3} {\sum_{vcc'}}' \mathrm{Re}\left[K^{\mathrm{ab}}_{cc'}\left(r^{\mathrm{c}}_{vc'} r^{\mathrm{d}}_{cv} + (c \leftrightarrow d)\right)\right] \delta(\omega - \omega_{cv}) \qquad \text{eq:mu} \quad (1)$$

where $K^{\mathrm{ab}}_{mn}(\mathbf{k}) = \sum_\ell v^{\mathrm{a}}_{nl}(\mathbf{k}) S^{\mathrm{b}}_{lm}(\mathbf{k})$ are the spin current matrix elements that, using time reversal invariance, $K^{\mathrm{ab}}_{nm}(-\mathbf{k}) = K^{\mathrm{ab}*}(\mathbf{k})$. The $'$ in the sum means that c and c' are quasi degenerate states and the sum only covers these states and since mu is real we have that $\mu^{\mathrm{abcd}}(\omega) =$

$\mu^{\mathrm{abdc}}(\omega)$.

Now we define the spin velocity, $\mathcal{V}^{\mathrm{ab}}(\omega,\alpha)$ as the speed at which the spin polarized in the b direction moves along the a direction when a normal incident beam reaches the xy plane with a polarization angle α. Then,

$$\mathcal{V}^{\mathrm{ab}}(\omega,\alpha) = \frac{2}{\hbar}\frac{\mu^{\mathrm{abxx}}(\omega)E^2(\omega)\cos^2(\alpha)+\mu^{\mathrm{abyy}}(\omega)E^2(\omega)\sin^2(\alpha)+2\mu^{\mathrm{abxy}}(\omega)E^2(\omega)\cos(\alpha)\sin(\alpha)}{\xi^{\mathrm{xx}}(\omega)E^2(\omega)\cos^2(\alpha)+\xi^{\mathrm{yy}}(\omega)E^2(\omega)\sin^2(\alpha)},$$
$$= \frac{2}{\hbar}\frac{\mu^{\mathrm{abxx}}(\omega)\cos^2(\alpha)+\mu^{\mathrm{abyy}}(\omega)\sin^2(\alpha)+\mu^{\mathrm{abxy}}(\omega)\sin(2\alpha)}{\xi^{\mathrm{xx}}(\omega)\cos^2(\alpha)+\xi^{\mathrm{yy}}(\omega)\sin^2(\alpha)}, \quad \text{eq:vab} \tag{2}$$

where $\xi^{\mathrm{aa}}(\omega)$ are the carrier generation rate tensor components[1]. For an angle $\alpha=\frac{\pi}{4}$ this expression can be reduced to

$$\mathcal{V}^{\mathrm{ab}}(\omega) = \frac{2}{\hbar}\frac{\mu^{\mathrm{abxx}}(\omega)+\mu^{\mathrm{abyy}}(\omega)+2\mu^{\mathrm{abxy}}(\omega)}{\xi^{\mathrm{xx}}(\omega)+\xi^{\mathrm{yy}}(\omega)}. \quad \text{eq:vab-90deg} \tag{3}$$

B. Fixing spin

sec:theory-fixspin

Considering that we have 2D structures, one of the options is fix the spin along the x, y, or z Cartesian coordinates. We define the magnitude of the spin velocity with spin polarization along the b direction as

$$|\mathcal{V}_{\sigma^{\mathrm{b}}}(\omega,\alpha)| = \sqrt{[\mathcal{V}^{\mathrm{ax}}(\omega,\alpha)]^2 + [\mathcal{V}^{\mathrm{ay}}(\omega,\alpha)]^2}, \quad \text{eq:vs-mag} \tag{4}$$

and the angle at which the spin velocity is directed on the xy plane as

$$\gamma_{\mathrm{b}}(\omega,\alpha) = \tan^{-1}\left(\frac{\mathcal{V}^{\mathrm{ay}}(\omega,\alpha)}{\mathcal{V}^{\mathrm{ax}}(\omega,\alpha)}\right), \quad \text{eq:gamma-ang} \tag{5}$$

where the angle is measured in the counter-clockwise direction from the positive x Cartesian coordinate. We also define two special angles

$$\gamma_{\mathrm{b}\parallel}(\omega,\alpha) = \alpha, \quad \text{eq:gammapar} \tag{6}$$
$$\gamma_{\mathrm{b}\perp}(\omega,\alpha) = \alpha \pm 90^\circ. \quad \text{eq:gammaperp} \tag{7}$$

The first corresponds to the case when the spin velocity is directed, on the xy plane in the same direction of the polarization angle of the incoming beam; the second one corresponds to the case when the spin velocity is directed perpendicularly respect to the polarization angle of the incoming beam.

C. Fixing velocity.

sec:theory-fixvel

In a similar way we can fix the velocity on the xy plane along x or y Cartesian coordinate and then define the magnitude of the spin velocity directed along the a direction as

$$|\mathcal{V}^{\mathrm{a}}(\omega,\alpha)| = \sqrt{[\mathcal{V}^{\mathrm{ax}}(\omega,\alpha)]^2+[\mathcal{V}^{\mathrm{ay}}(\omega,\alpha)]^2+[\mathcal{V}^{\mathrm{az}}(\omega,\alpha)]^2}, \quad \text{eq:vv-mag} \tag{8}$$

Then, the spin direction depends of the components of the previous equation and so we define the spin orientation polar and azimuthal angles as

$$\theta_{\mathrm{a}}(\omega,\alpha) = \cos^{-1}\left(\frac{\mathcal{V}^{\mathrm{az}}(\omega,\alpha)}{|\mathcal{V}^{\mathrm{a}}(\omega,\alpha)|}\right), \quad 0 \leq \theta \leq \pi, \quad \text{eq:polar-ang} \tag{9}$$

$$\varphi_{\mathrm{a}}(\omega,\alpha) = \tan^{-1}\left(\frac{\mathcal{V}^{\mathrm{ay}}(\omega,\alpha)}{\mathcal{V}^{\mathrm{ax}}(\omega,\alpha)}\right), \quad 0 \leq \varphi \leq 2\pi. \quad \text{eq:azimuthal-ang} \tag{10}$$

where $\theta_{\mathrm{a}}(\omega,\alpha)$ is measured from the positive to the negative z Cartesian coordinate and $\varphi_{\mathrm{a}}(\omega,\alpha)$ is measured on the xy plane in the counter-clockwise direction from the positive x Cartesian coordinate.

D. Layer-by-layer analysis.

sec:theory-layer

For a layered system we have that the total contribution of Eqns. (4) and (8) is given[1] by

Layer No.	Atom type	Position [Å] x	y	z
1	H	-0.61516	-1.42140	1.47237
2	C	-0.61516	-1.73300	0.39631
3	C	0.61516	1.73300	0.15807
4	C	0.61516	0.42201	-0.15814
5	C	-0.61516	-0.37396	-0.39632
6	H	-0.61516	-0.68566	-1.47237

TABLE I. Unit cell of *alt* structure. Layer division, atom types and positions for the *alt* structure. The structure unit cell was divided in six layers corresponding each one to atoms in different z positions. The corresponding layer atom position is depicted in Fig. 1 with the corresponding number of layer. tab:alt-unitcell

Layer No.	Atom type	Position [Å] x	y	z
1	H	-0.61516	-1.77416	0.73196
1	H	0.61518	0.35514	0.73175
2	C	-0.61516	-1.77264	-0.49138
2	C	-0.61516	-0.35600	-0.72316
2	C	0.61516	0.35763	-0.49087

TABLE II. Unit cell of *up* structure. Layer division, atom types and positions for the *up* structure. The structure unit cell was divided in two layers corresponding to hydrogen and carbon atoms.The corresponding layer atom position is depicted in Fig. 2 with the corresponding number of layer. tab:up-unitcell

$$|\mathcal{V}_{\sigma^{\mathrm{b}}}(\omega,\alpha)| = \ell_{\mathrm{eff}} \sum_{\ell=1}^{N_{\mathrm{eff}}} |\mathcal{V}_{\sigma^{\mathrm{b}}}(\ell|\omega,\alpha)| \quad \text{eq:vs-layer} \tag{11}$$

$$|\mathcal{V}^{\mathrm{a}}(\omega,\alpha)| = \ell_{\mathrm{eff}} \sum_{\ell=1}^{N_{\mathrm{eff}}} |\mathcal{V}^{\mathrm{a}}(\ell|\omega,\alpha)| \quad \text{eq:vv-layer} \tag{12}$$

III. RESULTS

sec:results

We preset the results for $|\mathcal{V}^{\mathrm{a}}(\omega,\alpha)|$ and $|\mathcal{V}_{\sigma^{\mathrm{b}}}(\omega,\alpha)|$ for the $C_{16}H_8$-alt and $C_{16}H_8$-up structures being both noncentrosymmetric semi-infinite 2D carbon systems with 50% hydrogenation in different arrangements. The *alt* system has alternating hydrogen atoms on the upper and bottom sides of the carbon sheet, while the *up* system has H only on the upper side. We take the hexagonal carbon lattice to be on the xy plane for both structures, and the carbon-hydrogen bonds on the perpendicular xz plane, as depicted in Figs. 1 and 2.

We calculated the self-consistent ground state and the Kohn-Sham states using density functional theory in the local density approximation (DFT-LDA) with a planewave basis using the ABINIT code[2]. We used Hartwigsen-Goedecker-Hutter (HGH) relativistic separable dual-space Gaussian pseudopotentials[3] including the spin-orbit interaction needed to calculate $\mu^{\mathrm{abcd}}(\omega,\alpha)$ presented in Eq. (1). The convergence parameters for the calculations of our results corresponding to the *alt* and *up* structures are cut-off energies of 65 Ha and 40 Ha, respectively. The energy eigenvalues and matrix elements for the *up* ad *alt* structures were calculated using 14452 **k** points and 8452 **k** points in the irreducible Brillouin zone (IBZ) presenting LDA energy band gaps of 0.72 eV and 0.088 eV, respectively. We notice that within DFT, the LDA is only one of other possible methods that can be used to determine the electronic structure of materials. Recent investigations on graphene show some of the differences in calculated values from several of these methods[4,5]. We note that the LDA is as good as these other approaches. It is also known that the DFT calculations predict a band gap for the material that differs from experiment. This can be corrected using other *ab initio* techniques, such as the GW approximation[6], but this calculation has a very high computational cost and is out of the scope in this paper. Even so, DFT still remains as an effective and useful tool for computing diverse properties derived from the electronic band structure.

A. Spin velocity

sec:res-spin_velocity

Using the Eq. (2), we calculated the $\mathcal{V}^{\mathrm{ab}}(\omega,\alpha)$ response for the *alt* and *up* 2D structures and for the CdSe and GaAs bulk systems and the results are presented in Fig. 3. The angle α presented in the response of each structure is that for which the response is maximized in

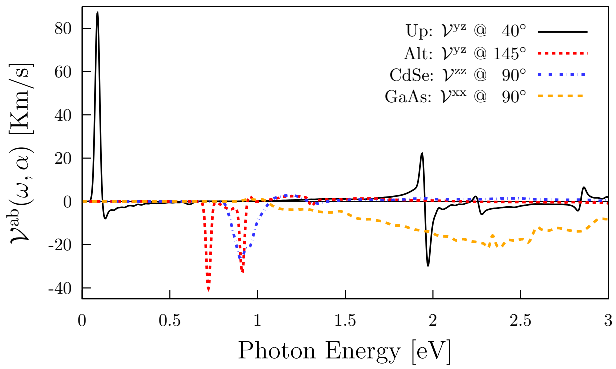

FIG. 3. Comparison of most intense responses of $\mathcal{V}^{ab}$ for 2D *alt* and *up*, and bulk CdSe and GaAs structures and the corresponding polarization angles. fig:vab-str-comp

each case. From the figure we have that the onset of the response starts when the energy of the incoming beam is the same of the gap energy. The most intense response corresponds to the *up* structure centered at 0.088 eV corresponding to the Far Infrared (FIR) radiation and reaching a spin velocity of 87.2 Km/s. In the other hand, for an energy range from 0.66 eV to 3.0 eV, corresponding to energies of the Near Infrared (NIR) and visible radiation, all the four structures have contributions in the same order of magnitude. Starting with the 2D structures we have that the *up* structure has other two peaks centered at 1.94 eV and 1.97 eV reaching spin velocities of 22.2 Km/s and -29.7 Km/s, respectively, and the *alt* structure has two peaks centered at 0.72 eV and 0.91 eV reaching spin velocities of -40.2 Km/s and -32.9 Km/s, respectively. Then, for the bulk structures we have that the

Structure	Kind of system	Pol. Ang.	Energy [eV]	$\mathcal{V}^{ab}(\omega,\alpha)$ ab	[Km/s]
up	2D	40	0.09	yz	87.16
			1.94	yz	22.22
			1.97	yz	-29.70
alt	2D	145	0.72	yz	-40.21
			0.91	yz	-32.89
CdSe	bulk	90	0.91	zz	-26.87
GaAs	bulk	90	2.31	xx	-21.62

TABLE III. Comparison of the reported maxima values of $\mathcal{V}^{ab}$ for different structures and the corresponding polarization angle α and energy values. tab:vab-str-comp

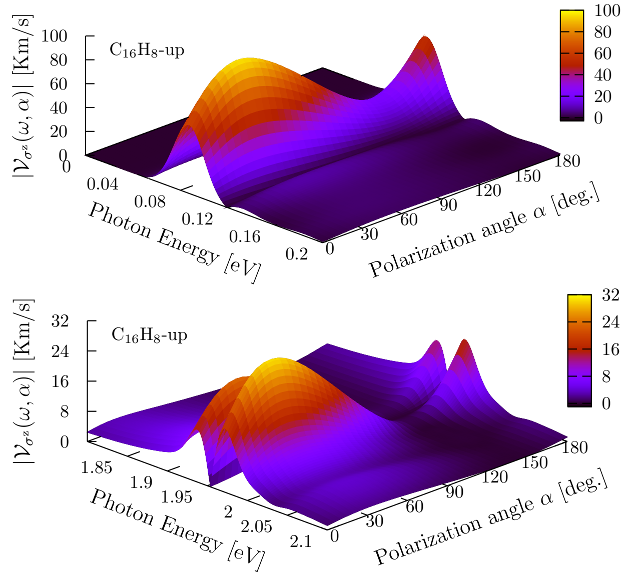

FIG. 4. $|\mathcal{V}_{\sigma^z}(\omega,\alpha)|$ response as a function of the photon energy and polarization angle α for the *up* structure for two energy ranges. The absolute maxima is located for an energy range from 0.08 eV to 0.10 eV, in the Far Infrared radiation range, and two local maxima from 1.90 eV to 1.93 eV and from 1.96 eV to 2.0 eV, in the visible radiation range, all for polarization angles between 25° and 50°. fig:up-3d-vsz

CdSe has only one intense response centered at 0.91 eV reaching a spin velocity of -26.9 Km/s, and the GaAs structure has a large and almost planar zone where the response is held reaching the maximum for an incoming beam of energy of 2.31 eV and resulting in a spin velocity of -21.6 Km/s. A negative quantity in the spin velocity means a change in the spin polarization traveling in the opposite direction. In table III we present the comparison of this values for the 2D and bulk structures. We found that the most intense response for the spin velocity of the *up* structure is 3.25 times more intense than CdSe and 4.03 times more intense than the GaAs bulk structures. Also, the *alt* structure has a response more intense than the bulk systems but being less intense than the corresponding to the *up* one.

B. Fixing spin

sec:res-fixspin

Using the Eq. (4), we calculated the $|\mathcal{V}_{\sigma^b}|(\omega,\alpha)$ response and made the analysis for

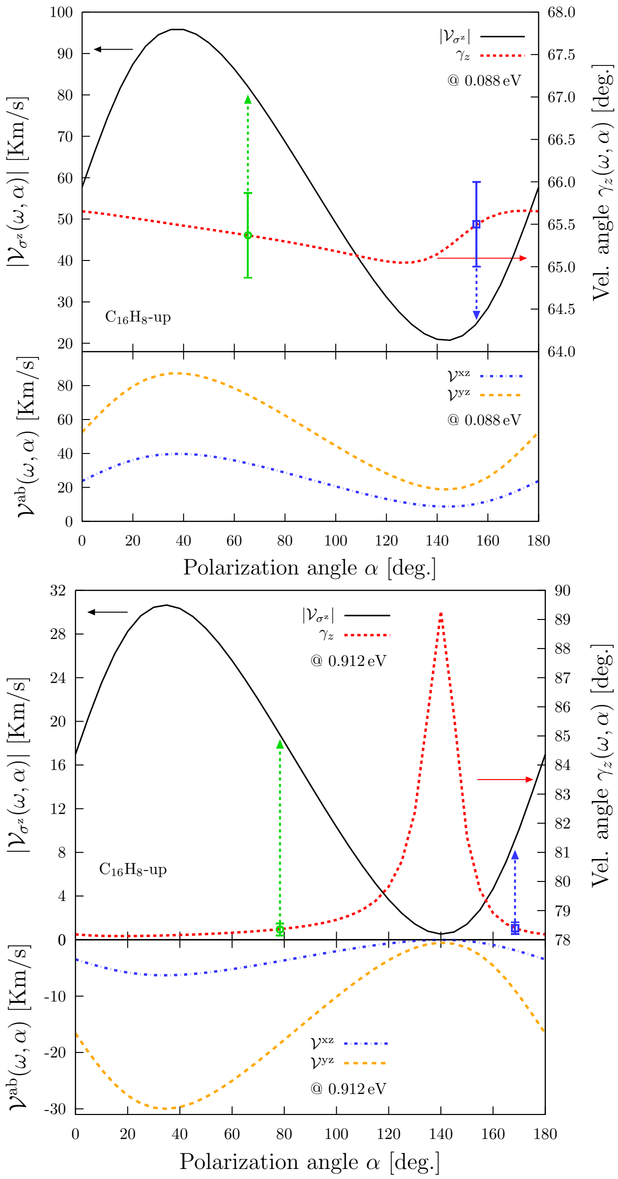

FIG. 5. Most intense response of $|\mathcal{V}_{\sigma^z}(\omega,\alpha)|$ (top frames, right scale of figs (a) and (b)), the corresponding velocity angle $\gamma_z(\omega,\alpha)$ (top frames, right scale), the collinear (circled box) and perpendicular (square box) angles, and the two components $\mathcal{V}^{xz}(\omega,\alpha)$ and $\mathcal{V}^{yz}(\omega,\alpha)$ (bottom frames) for the *up* structure fixing the energy to 0.088 eV. `fig:up-vaz-rag`

the case when the spin is fixed in the z direction, directed perpendicularly to the surface of the *alt* and *up* structures. Also, using the Eq. (5), we determined the angle $\gamma_b(\omega,\alpha)$ where the spin-velocity is directed on the surface of the each structure.

Up structure

The most interesting case is that for which the spin is perpendicular to the surface corresponding to $\mathcal{V}^{xz}(\omega,\alpha)$. For this case we first analyzed two energy ranges for the *up* structure, the first for an incoming energy beam from 0.0 eV to 0.2 eV which include the THz and the Mid Infrared (MIR) range, where the absolute maximum of the $|\mathcal{V}_{\sigma^z}(\omega,\alpha)|$ response is obtained and the second for an energy range from 1.80 eV to 2.1 eV, corresponding to visible radiation, where two local maxima are found. In Fig. 4 we present the $|\mathcal{V}_{\sigma^z}(\omega,\alpha)|$ spectra resulting from evaluate Eq. (4). Making the analysis, we obtained that the zone where the maximum response is held corresponds to a energy range of the incident beam from 0.084 eV to 0.093 eV and polarization angles α between 30° and 45°. Also two local maxima are held for same polarization angles but for an energy range of the incoming beam between 1.90 eV and 2.05 eV. In the top frames of top and bottom panels of Fig. 5 we present in solid lines the result of evaluate $|\mathcal{V}_{\sigma^z}(\omega,\alpha)|$, related to the left scale, fixing the energy of the incoming beam to 0.088 eV and 0.912 eV, respectively, for which value the response is maximized for the *up* structure. In the same panels and frames we present in dashed lines, related to the right scale, the corresponding velocity angle $\gamma_z(\omega,\alpha)$ obtained from evaluate Eq. (5), and in the bottom frames the panels we present the corresponding components $\mathcal{V}^{xz}(\omega,\alpha)$ and $\mathcal{V}^{yz}(\omega,\alpha)$. Also we present two circled and square boxes indicating the values where the angles of the spin velocity are parallel (Eq. 6) and perpendicular (Eq. 7) and the arrows are directed to the value of the response corresponding to those angles. From top panels of Figs. 4 and 5 we have that the absolute maximum response for the *up* structure is obtained for an incoming beam with energy of 0.088 eV and polarization angle $\alpha = 40°$ resulting in a value of $|\mathcal{V}_{\sigma^z}(\omega,\alpha)| = 95.8$ Km/s coming from the contribution of the components $\mathcal{V}^{xz}(\omega,\alpha) = 39.8$ Km/s and $\mathcal{V}^{yz}(\omega,\alpha) = 87.2$ Km/s for the spin polarized in the z direction and having a velocity angle $\gamma_z(\omega,\alpha) = 65°$ on the xy plane. From the top panel of Fig. 5 we have that the velocity angle is almost constant for all the polarization angle range having values of $\gamma_z(\omega,\alpha) = 65.5° \pm 0.5°$. In this panel the green circled box indicates the value for which the polarization angle and the response direction angle are collinear (Eq. 6) being $\gamma_{z\|}(\omega,\alpha) = 65.5°$ and resulting in a value of the response of $|\mathcal{V}_{\sigma^z}(\omega,\alpha)| = 82.3\,\mathrm{Km/s}$ indicated by the upward green arrow. Also the blue square box indicates the value for which the polarization angle and the response angle are perpendicular being $\alpha = 155.5°$ and $\gamma_{z\perp}(\omega,\alpha) = 65.5°$; for this angle the response has a value of $|\mathcal{V}_{\sigma^z}(\omega,\alpha)| = 24.8\,\mathrm{Km/s}$ indicated by the blue downward arrow. Now, from bottom panels of Figs. 4 and 5 we have that a local maximum of the response is obtained for an incoming beam with energy of 0.912 eV and same polarization angle $\alpha = 40°$ resulting in a value of $|\mathcal{V}_{\sigma^z}(\omega,\alpha)| = 30.3\,\mathrm{Km/s}$. This comes from a major contribution of the $\mathcal{V}^{\mathrm{yz}}(\omega,\alpha)$ component being directed in a velocity angle $\gamma_z(\omega,\alpha) = 78°$ on the first Cartesian Quadrant on the xy plane, for the spin polarized in the z direction. Again from the bottom panel of Fig. 5 we found that the velocity angle is almost constant at 78° and has variations of 1° for polarization angles between 0° and 100°. In this range the green circled box indicates the value for which the polarization angle and the response direction angle are collinear corresponding to $\gamma_{z\|}(\omega,\alpha) = 78.5°$ and having a response value of $|\mathcal{V}_{\sigma^z}(\omega,\alpha)| = 23.5\,\mathrm{Km/s}$ indicated with the green upward arrow. Finally, the blue square box indicates the value for which the polarization angle and the response angle are perpendicular being $\alpha = 168.5°$ $\gamma_{z\perp}(\omega,\alpha) = 78.5°$ and having a response $|\mathcal{V}_{\sigma^z}(\omega,\alpha)| = 9.0\,\mathrm{Km/s}$ indicated with the blue upward arrow. We also made the analysis for the cases when the spin polarization is directed along the x and y Cartesian coordinates but we do not present here the corresponding plots. For those cases we have that the absolute maxima responses are obtained for an energy of the incoming beam equal to 0.088 eV and polarization angle $\alpha = 40°$ resulting in values of $|\mathcal{V}_{\sigma^x}(\omega,\alpha)| = 37.4\,\mathrm{Km/s}$ and $|\mathcal{V}_{\sigma^y}(\omega,\alpha)| = 24.8\,\mathrm{Km/s}$.

Alt structure

For the *alt* structure we analyzed the energy range for the incident beam from 0.6 eV to 1.0 eV, corresponding to the NIR radiation, where the absolute maximum of $|\mathcal{V}_{\sigma^z}(\omega,\alpha)|$ response is obtained. In Fig. 6 we present the $|\mathcal{V}_{\sigma^z}(\omega,\alpha)|$ spectra for the *alt* structure. From Figs. 6 and 7 we have that the absolute maximum response is obtained for an incoming beam with polarization angle $\alpha = 145°$ reaching a velocity of $|\mathcal{V}_{\sigma^z}(\omega,\alpha)| = 43.0\,\mathrm{Km/s}$ for the spin polarized in the z direction and resulting in a velocity angle $\gamma_z(\omega,\alpha) = 50°$ on the first Cartesian

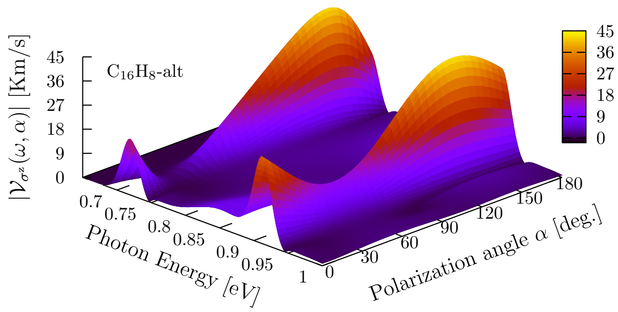

FIG. 6. $|\mathcal{V}_{\sigma^z}(\omega,\alpha)|$ response as a function of the photon energy and polarization angle α for the *alt* structure. The local and the absolute maxima are located in the energy ranges from 0.67 eV to 0.73 eV and from 0.90 eV to 0.93 eV, respectively, and both in the Near Infrared and for polarization angles between 120° and 150°. `fig:alt-3d-vsb`

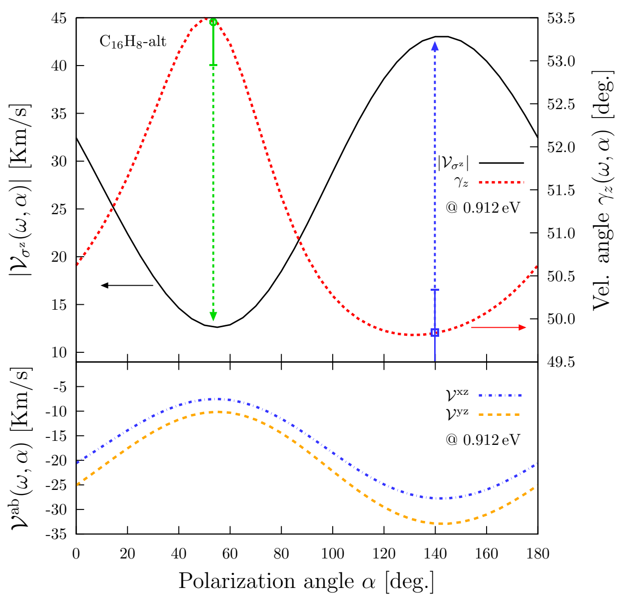

FIG. 7. Most intense response of $|\mathcal{V}_{\sigma^z}(\omega,\alpha)|$ (top frame, left scale) the corresponding velocity angle $\gamma_z(\omega)$ (top frame, right scale), the collinear (circled box) and perpendicular (square box) angles, and the two components $\mathcal{V}^{\mathrm{xz}}(\omega)$ and $\mathcal{V}^{\mathrm{yz}}(\omega)$ (bottom frame) for the *alt* structure fixing the energy to 0.912 eV. `fig:alt-vaz-rag`

Quadrant of the xy plane. Also, from the top frame of Fig. 7 we found that the velocity angle has small variations being centered at 51.5° and having variations of ±2° for the polarization angle range $0^\circ \leq \alpha \leq 180^\circ$. Again the circled box indicates the collinear angle (Eq. (6)) corresponding to $\gamma_{\mathrm{z}\|}(\omega, \alpha) = 53.5^\circ$ corresponding a value of $|\mathcal{V}_{\sigma^{\mathrm{z}}}(\omega, \alpha)| = 12.7\,\mathrm{Km/s}$; the blue square box indicates the perpendicular angles corresponding values $\alpha = 140^\circ$ and $\gamma_{\mathrm{z}\perp}(\omega, \alpha) = 50^\circ$ with a value of $|\mathcal{V}_{\sigma^{\mathrm{z}}}(\omega, \alpha)| = 43\,\mathrm{Km/s}$. Again, for the cases in which the spin polarization is parallel to the surface of the *alt* structure was calculated but the plots are not presented here. The absolute maxima for the case when the spin polarization is directed in the x and y direction are obtained for an energy of the incoming beam equal to 0.912 eV and polarization angle $\alpha = 145^\circ$ resulting in values of $|\mathcal{V}_{\sigma^{\mathrm{x}}}(\omega, \alpha)| = 27.1\,\mathrm{Km/s}$ and $|\mathcal{V}_{\sigma^{\mathrm{y}}}(\omega, \alpha)| = 33.2\,\mathrm{Km/s}$.

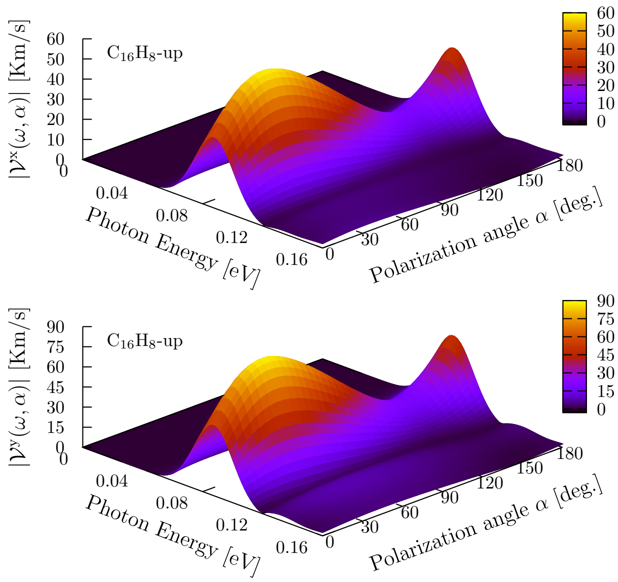

FIG. 8. $|\mathcal{V}^{\mathrm{x}}(\omega, \alpha)|$ and $|\mathcal{V}^{\mathrm{y}}(\omega, \alpha)|$responses as a function of the photon energy and polarization angle α for the *up* structure. The absolute maxima of both are localized in the energy range from 0.08 eV to 0.10 eV, in the Far Infrared, and for polarization angles from 25° to 50°. `fig:up-3d-vva-1`

C. Fixing velocity

`sec:res-fixvel`

Now, using the Eq. (8), we calculated the $|\mathcal{V}^{\mathrm{a}}(\omega, \alpha)|$ response and made the analysis for the case when the velocity is fixed in the x and y direction over the surface of the *alt* and *up* structures. Also, using the Eqns. (9) and (10), we determined the polar $\theta_{\mathrm{a}}(\omega, \alpha)$ and azimuthal $\varphi_{\mathrm{a}}(\omega, \alpha)$ angles where the spin polarization is directed.

Up structure.

In top and bottom panels of Fig. 8 we present $|\mathcal{V}^{\mathrm{x}}(\omega, \alpha)|$ and $|\mathcal{V}^{\mathrm{y}}(\omega, \alpha)|$ resulting from evaluate the Eq. (8) in the energy range from 0.00 eV to 0.16 eV for the *up* structure. From this figure we can see that for the zone between the energy range of 0.084 eV-0.093 eV and polarization angles between 30° and 45° is the zone where the maximum response is held for both, $|\mathcal{V}^{\mathrm{x}}(\omega, \alpha)|$ and $|\mathcal{V}^{\mathrm{y}}(\omega, \alpha)|$.

In the top frames of top and bottom panel of Fig. 9 we present in solid lines the results of $|\mathcal{V}^{\mathrm{x}}(\omega, \alpha)|$ and $|\mathcal{V}^{\mathrm{y}}(\omega, \alpha)|$, related to the left scale, fixing the polarization angle to $\alpha = 40^\circ$ for which the response is maximized. In the same panels and frames we present in dashed lines the corresponding polar $\theta_a(\omega, \alpha)$ and azimuthal $\varphi_a(\omega, \alpha)$ spin angles related to the right scale. Also, in the bottom frames we present the corresponding components $\mathcal{V}^{\mathrm{xx}}(\omega, \alpha)$, $\mathcal{V}^{\mathrm{xy}}(\omega, \alpha)$, $\mathcal{V}^{\mathrm{xz}}(\omega, \alpha)$, and $\mathcal{V}^{\mathrm{yx}}(\omega, \alpha)$, $\mathcal{V}^{\mathrm{yy}}(\omega, \alpha)$, $\mathcal{V}^{\mathrm{yz}}(\omega, \alpha)$. From the top panel of Fig. 9 we have that for an incoming bean of energy 0.088 eV the three components have similar contributions with values of $\mathcal{V}^{\mathrm{xx}}(\omega, \alpha) = -36.5\,\mathrm{Km/s}$, $\mathcal{V}^{\mathrm{xy}}(\omega, \alpha) = -23.2\,\mathrm{Km/s}$, and $\mathcal{V}^{\mathrm{xz}}(\omega, \alpha) = 39.8\,\mathrm{Km/s}$ resulting in a response $|\mathcal{V}^{\mathrm{x}}(\omega, \alpha)| = 58.7\,\mathrm{Km/s}$ being this value the absolute maximum obtained when the spin-velocity is fixed in the x direction. To this value corresponds the polar and azimuthal spin angles of $\theta_{\mathrm{x}}(\omega, \alpha) = 47$ and $\varphi_{\mathrm{x}}(\omega, \alpha) = 212$, respectively, being directed upper the third Cartesian Quadrant of the xy plane. Also from this figure we have that those angle values are held for almost all the peak of the response having a variation of ±2°. Now, from the bottom panel of Fig. 9 we have that the yx and yy components have less contributions for the total response than the yz and for the same incoming beam energy the components have values of $\mathcal{V}^{\mathrm{yx}}(\omega, \alpha) = -7.9\,\mathrm{Km/s}$ $\mathcal{V}^{\mathrm{yy}}(\omega, \alpha) = 8.6\,\mathrm{Km/s}$, and $\mathcal{V}^{\mathrm{yz}}(\omega, \alpha) = 87.2\,\mathrm{Km/s}$ resulting in a re-

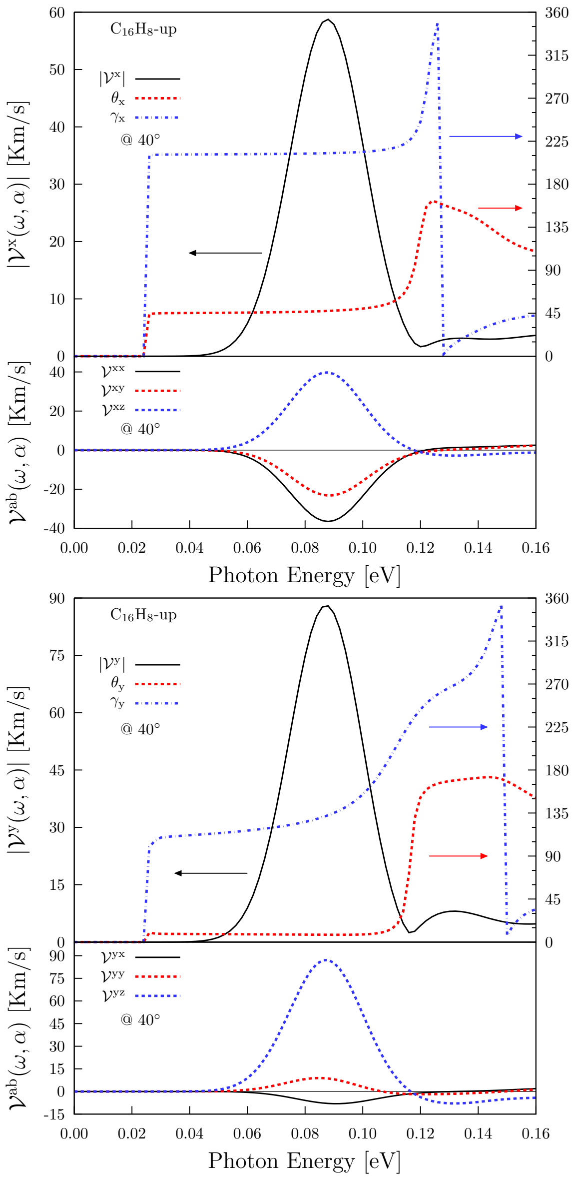

FIG. 9. Most intense response of $|\mathcal{V}^{\mathrm{x}}(\omega,\alpha)|$ and $|\mathcal{V}^{\mathrm{y}}(\omega,\alpha)|$ (top frames left scale of Figs. (a) and (b)), the corresponding polar φ and azimuthal θ angles (top frames right scale), and the corresponding three components (bottom frames) for the *up* structure fixing the polarization angle to $\alpha = 40°$ to maximize the response. `fig:up-vab-comp-rtp-1`

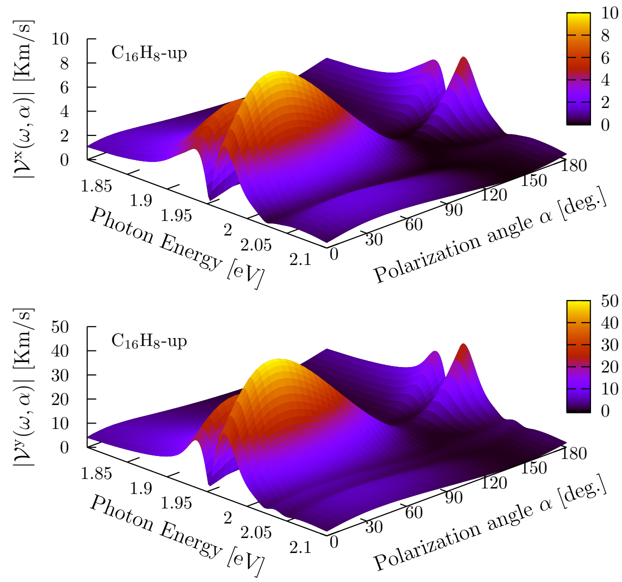

FIG. 10. $|\mathcal{V}^{\mathrm{x}}(\omega,\alpha)|$ (top panel) and $|\mathcal{V}^{\mathrm{y}}(\omega,\alpha)|$ (bottom panel) as a function of the photon energy and polarization angle α for the *up* structure. Two local maxima of both responses are localized in the energy range from 1.90 eV to 1.93 eV and from 1.96 eV to 2.0 eV, in the visible radiation range, and for polarization angles between 25° and 50°`fig:up-3d-vva-2`

sponse $|\mathcal{V}^{\mathrm{y}}(\omega,\alpha)| = 87.9\,\mathrm{Km/s}$. This value is the absolute maximum obtained when the spin-velocity is fixed in the y direction and is 1.5 times more intense than $|\mathcal{V}^{\mathrm{x}}(\omega,\alpha)|$. For this absolute maximum corresponds spin polar and azimuthal angles $\theta_{\mathrm{y}}(\omega,\alpha) = 8°$ and $\varphi_{\mathrm{y}}(\omega,\alpha) = 133°$ being directed the spin almost perpendicularly over the xy plane and localized on the first Cartesian Quadrant. In a different way than in the $|\mathcal{V}^{\mathrm{x}}(\omega,\alpha)|$ case only the polar angle is hold at 8° for the peak of the response having variations of ±2° but the azimuthal angle changes from 99° to 176° having a value of 133° for the maximum. We also found that since the onset of the response till an energy for the incoming beam of 0.118 eV the components of both responses, $|\mathcal{V}^{\mathrm{x}}(\omega,\alpha)|$ and $|\mathcal{V}^{\mathrm{y}}(\omega,\alpha)|$, have no change in the spin polarization direction. Finally, after this energy value the responses go to zero. Also there is another energy range of interest for an incoming energy beam from 1.80 eV to 2.10 eV, corresponding to visible radiation, presented in Fig. 10 where two local maxima of $|\mathcal{V}^{\mathrm{x}}(\omega,\alpha)|$ and $|\mathcal{V}^{\mathrm{y}}(\omega,\alpha)|$ are obtained for the *up* structure. We found that the two local maxima are obtained for an energy of the incident beam energies of 1.934 eV and 1.972 eV fixing again the polarization angle to 40°. In the top frames of top and bottom panels of Fig. 11 we present in solid lines the results of $|\mathcal{V}^{\mathrm{x}}(\omega,\alpha)|$ and $|\mathcal{V}^{\mathrm{y}}(\omega,\alpha)|$, related to the left scale, fixing the polarization angle to $\alpha = 40°$ for which the response is maxi-

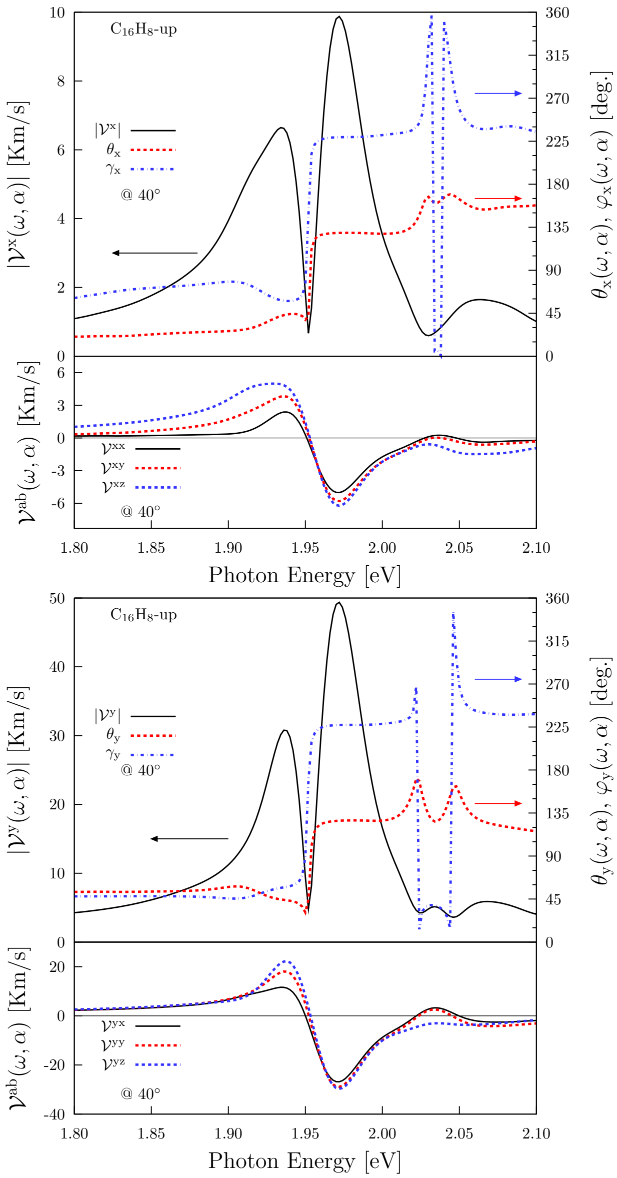

FIG. 11. Intense response of $|\mathcal{V}^{\rm x}(\omega,\alpha)|$ and $|\mathcal{V}^{\rm y}(\omega,\alpha)|$ (top frames left scale of Figs. (a) and (b)), the corresponding polar φ and azimuthal θ angles (top frames right scale), and the corresponding three components (bottom frames) for the *up* structure fixing the polarization angle to $\alpha = 40°$ to maximize the response. fig:up-vab-comp-rtp-2

mized for the *up* structure. In the same panels and frames we present in dashed lines the corresponding polar ($\theta_{\rm x}(\omega,\alpha)$ and $\theta_{\rm y}(\omega,\alpha)$) and azimuthal ($\varphi_{\rm x}(\omega,\alpha)$ and $\varphi_{\rm y}(\omega,\alpha)$) angles related to the right scale and In the bottom frames the corresponding response components. We found that for both cases the components have similar contributions for the corresponding response and for an incoming energy beam of 1.934 eV we have the first local maximum resulting in a value of $|\mathcal{V}^{\rm x}(\omega,\alpha)| = 6.6$ Km/s along the x direction with polar and azimuthal spin polarization angles $\theta_{\rm x}(\omega,\alpha) = 42°$ and $\varphi_{\rm x}(\omega,\alpha) = 59°$ being the spin directed over the first Cartesian Quadrant of the xy plane. For the spin moving along the y direction we have a value of $|\mathcal{V}^{\rm y}(\omega,\alpha)| = 28.7$ Km/s with polar and azimuthal angles $\theta_{\rm y}(\omega,\alpha) = 45°$ and $\varphi_{\rm y}(\omega,\alpha) = 56°$ being the spin directed over the first Cartesian Quadrant of the xy plane. Alike, for an incoming energy beam of 1.972 eV we found the second and more intense local maxima for which all the components have similar contributions for the corresponding response resulting in values of $|\mathcal{V}^{\rm x}(\omega,\alpha)| = 9.9$ Km/s and spin polarization angles $\theta_{\rm x}(\omega,\alpha) = 129°$ and $\varphi_{\rm x}(\omega,\alpha) = 229°$ being the spin directed downward the third Cartesian Quadrant of the xy plane. For the spin moving in the y direction we have a value of $|\mathcal{V}^{\rm y}(\omega,\alpha)| = 49.4$ Km/s with spin polarization angles $\theta_{\rm y}(\omega,\alpha) = 127°$ and $\varphi_{\rm y}(\omega,\alpha) = 227°$ and the spin being directed downward the third Cartesian Quadrant of the xy plane. Also all the components of the responses keep the spin polarization positive till an energy of the incoming beam equal to 1.954 eV when the spin polarization ad current changes the direction and after an energy for the incoming beam equal to 2.05 eV both responses goes to zero.

Alt structure.

For the *alt* structure we analyzed the energy range from 0.6 eV to 1.0 eV, corresponding to the NIR radiation, where we found a local maxima and the most intense responses for $|\mathcal{V}^{\rm x}(\omega,\alpha)|$ and $|\mathcal{V}^{\rm a}(\omega,\alpha)|$; the corresponding spectra is shown in Fig. 12. From this figure we can see that for the zone between the energy range of 0.90 eV-0.93 eV and polarization angles between 120° and 150° is the zone where the maximum for both responses is held. In the top frames of top and bottom panels of Fig. 13 we present the spectra of $|\mathcal{V}^{\rm x}(\omega,\alpha)|$ and $|\mathcal{V}^{\rm y}(\omega,\alpha)|$, related to the left scale, fixing the polarization angle to $\alpha = 145°$. In the same figures and frames we present the spin polarization angles related to the right scale and in the bottom frames the corresponding three components. Making the analysis for the components and angles when the spin current is directed in

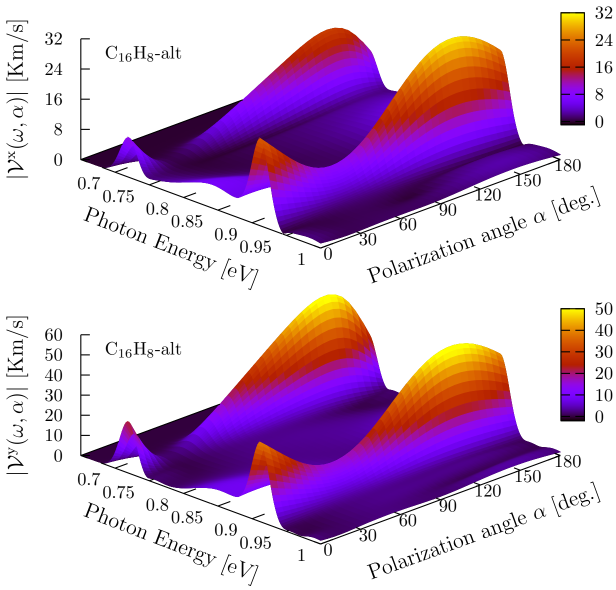

FIG. 12. $|\mathcal{V}^{x}(\omega,\alpha)|$ (top panel) and $|\mathcal{V}^{y}(\omega,\alpha)|$ (bottom panel) as a function of the photon energy and polarization angle α for the *alt* structure. The local and the absolute maxima are located in the energy ranges from 0.67 eV to 0.73 eV and from 0.90 eV to 0.93 eV, respectively, and both in the Near Infrared and for polarization angles between 120° and 150°. `fig:alt-3d-vva`

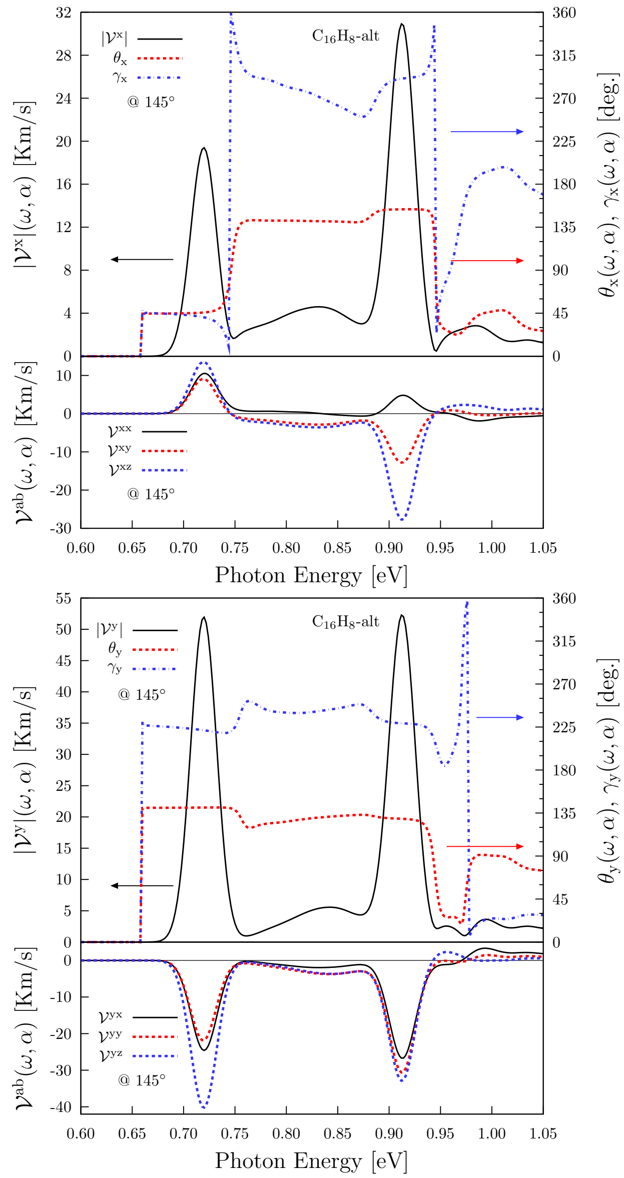

FIG. 13. Most intense response of $|\mathcal{V}^{x}(\omega,\alpha)|$ and $|\mathcal{V}^{y}(\omega,\alpha)|$ (top frames left scale of Figs. (a) and (b)), the corresponding polar φ and azimuthal θ angles (top frames right scale), and the corresponding three components (bottom frames) for the *alt* structure fixing the polarization angle to $\alpha = 145°$ to maximize the response. `fig:alt-vab-comp-rtp`

the x direction, corresponding to the top panel of Fig. 13, we found that when the energy of the incoming beam is 0.720 eV we have similar contributions from all the components resulting in a response of $|\mathcal{V}^{x}(\omega,\alpha)| = 19.4$ Km/s and polar and azimuthal spin polarization angles $\theta_x(\omega,\alpha) = 46°$ and $\varphi_x(\omega,\alpha) = 41°$ being the spin directed over the first Cartesian Quadrant of the xy plane; then, for an energy of 0.912 eV we have a major contribution from the $\mathcal{V}^{xz}(\omega,\alpha)$ component resulting in a total response of $|\mathcal{V}^{x}(\omega,\alpha)| = 30.9$ Km/s being this value the absolute maximum when the spin velocity is directed in the x Cartesian direction. The corresponding polar and azimuthal angles are $\theta_x(\omega,\alpha) = 154°$, and $\varphi_x(\omega,\alpha) = 290°$ being the spin directed downward the fourth Cartesian Quadrant of the xy plane. Making now the analysis for the components and angles when the spin current is directed along the y direction, corresponding to the bottom panel of Fig. 13, we found that when the energy of the incoming beam is 0.720 eV we have more contribution from the $\mathcal{V}^{yz}(\omega,\alpha)$ component and the response has a value of $|\mathcal{V}^{y}(\omega,\alpha)| = 51.9$ Km/s corresponding the polar and azimuthal angles $\theta_y(\omega,\alpha) = 141°$ and $\varphi_y(\omega,\alpha) = 222°$ being the spin directed downward the third Cartesian Quadrant of the xy plane. For the peak centered at 0.912 eV we have similar contributions of all the components resulting in a response $|\mathcal{V}^{y}(\omega,\alpha)| = 52.3$ Km/s being this the absolute maximum response for the *alt* structure. The corresponding angles are $\theta_{\rm y}(\omega,\alpha) = 129^\circ$ and $\varphi_{\rm y}(\omega,\alpha) = 229^\circ$ being the spin directed downward the third Cartesian Quadrant of the xy plane. Finally we have that the three components of $|\mathcal{V}^{\rm y}|$ are negative keeping the same spin polarization and velocity direction since the onset of the response to a energy of the incoming beam of 0.886 eV when the response decreases and goes to zero.

IV. LAYER-BY-LAYER ANALYSIS

`sec:res-layer_by_layer_analysis`

The structures presented here where divided into layers to analyze the he layer-by-layer contribution for $\mathcal{V}^{\rm ab}$ response. The *alt* structure was divided in six layers corresponding the first one to the top hydrogen atoms, from the second to the forth to carbon atoms in different z positions, and the sixth and last one to the bottom hydrogen atoms. The *up* structure was divided into two layers, the first one comprised by the top hydrogen atoms and the second by the carbon atoms. The layer divisions and atom positions for the unit cells are shown in Tables I and II.

From the bottom frames of Figs. 9 and 11 we can see that for the *up* structure again the most intense component of $|\mathcal{V}^{\rm x}|$ and $|\mathcal{V}^{\rm y}|$ corresponds to $\mathcal{V}^{\rm yz}$ which has a value of 87.2 Km/s for an energy incident beam of 0.088 eV and -29.7 Km/s for an energy incident beam of 1.972 eV. This component and the corresponding layer by layer contribution is depicted in Fig. 14s. From this figure we have that for the energy range from 0 eV to 0.2 eV the response comes from the second layer composed by carbon atoms presented in Tab. II and denoted by the number 2 in Fig. 2. In the other hand, the response for the energy range from 1.8 eV to 2.1 eV almost all the response comes from the carbon atoms having a leaser contribution from the hydrogen layer. From the bottom frames of Fig. 13 we can see that for the *alt* structure the most intense component of $|\mathcal{V}^{\rm x}|$ and $|\mathcal{V}^{\rm y}|$ corresponds to $\mathcal{V}^{\rm yz}$ which has a value of -40.2 Km/s for an energy incident beam of 0.72 eV. This component and the corresponding layer by layer contribution is depicted in Fig. 15. From this figure we have that for the energy range from 0.70 eV to 0.74 eV the fifth

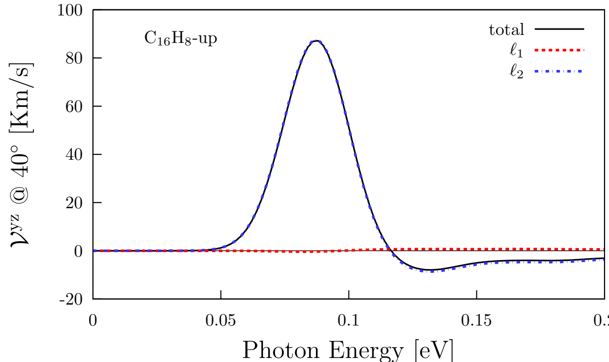

`fig:up-vyz-lay-1`

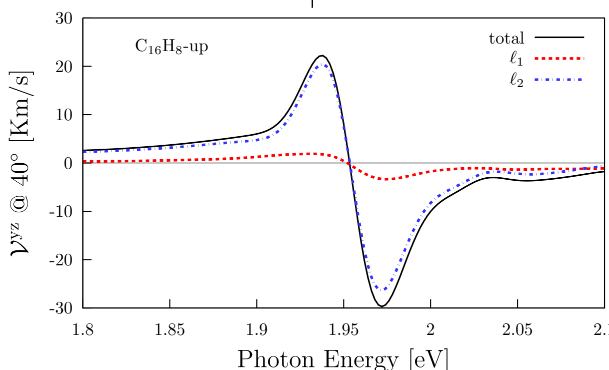

`fig:up-vyz-lay-2`

FIG. 14. Layer-by-layer contribution of $\mathcal{V}^{\rm yz}$ for the *up* structure. `fig:up-vyz-lay`

and sixth layers corresponding to the bottom carbon and hydrogen numbered with 5 and 6 in Fig. 1 have contributions in opposite direction than the other 4 layers resulting in a total response $\mathcal{V}^{\rm yz} = -40.2$ Km/s for an incoming beam energy of 0.72 eV. In the other hand, for the energy range from 0.88 eV to 0.95 eV the response for the all six layers the responses are in the same direction resulting in a total response $\mathcal{V}^{\rm yz} = -32.89$ Km/s for an incoming beam with energy of 0.912 eV.

[1] N. Arzate, R. A. Vázquez-Nava, and B. S. Mendoza, Phys. Rev. B **90**, 205310 (2014).

[2] X. Gonze, B. Amadon, P.-M. Anglade, J.-M. Beuken, F. Bottin, P. Boulanger, F. Bruneval, D. Caliste, R. Caracas, M. Côté, T. Deutsch, L. Genovese, P. Ghosez, M. Giantomassi,

S. Goedecker, D. Hamann, P. Hermet, F. Jollet, G. Jomard, S. Leroux, M. Mancini, S. Mazevet, M. Oliveira, G. Onida, Y. Pouillon, T. Rangel, G.-M. Rignanese, D. Sangalli, R. Shaltaf, M. Torrent, M. Verstraete, G. Zerah, and J. Zwanziger, Comput. Phys. Commun. **180**, 2582 (2009).
[3] C. Hartwigsen, S. Goedecker, and J. Hutter, Phys. Rev. B **58**, 3641 (1998).
[4] P. Karamanis, N. Otero, and C. Pouchan, J. Phys. Chem. C **119**, 11872 (2015).
[5] A. R. Botello-Méndez, S. M. Dubois, A. Lherbier, and J. C. Charlier, Acc. Chem. Res. **47**, 3292 (2014).
[6] G. Onida, L. Reining, and A. Rubio, Rev. Mod. Phys. **74**, 601 (2002). LastBibItem

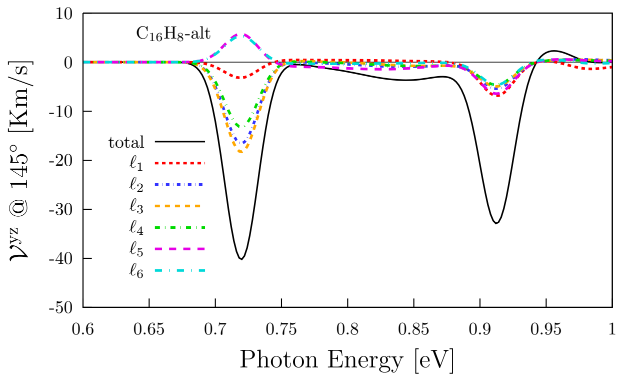

FIG. 15. Layer-by-layer contribution of $\mathcal{V}^{\mathrm{yz}}$ for the *alt* structure. fig:alt-vyz-lay